Temperature dependent hot electron transport in slightly lattice mismatched AlInN/AlN/GaN heterostructures

AYKUT ILGAZ[a], SIBEL GÖKDEN[a*], REMZIYE TÜLEK[a], ALI TEKE[a], SÜLEYMAN ÖZÇELIK[b], EKMEL ÖZBAY[c]
[a] *Department of Physics, Faculty of Science and Letter, Balıkesir University, Çağış Kampüsü, 10145 Balıkesir, Turkey*
[b] *Department of Physics, Faculty of Science and Letter, Gazi University, Teknikokullar, 06500 Ankara, Turkey*
[c] *Department of Physics, Department of Electrical and Electronics Engineering, Nanotechnology Research Center-NANOTAM, Bilkent University, 06800 Ankara, Turkey*

In this work, the hot-electron transport properties of AlInN/AlN/GaN HEMT structures with a high sheet electron density of 4.84×10^{13} cm^{-2} grown by MOCVD (Metal Organic Chemical Vapor Deposition) on sapphire substrate were investigated at lattice temperature ranging from 10 K to 300 K. High speed current–voltage measurements and Hall measurements were used to study hot-electron transport. Current-voltage characteristics show that current and drift velocity increase linearly but deviate from the linearity towards high voltages, as would be expected from the increased scattering of hot electrons with LO phonons. However, no saturation of current and drift velocity were observed at the highest voltage reached. Drift velocities were deduced as approximately 6.7×10^{6} and 6.1×10^{6} cm/s at an electric field of around E ~ 23 kV/cm at lattice temperatures T_L = 10 K and 300 K, respectively. To obtain the electron temperature as a function of the applied electric field and power loss as a function of the electron temperature, the so-called mobility comparison method with power balance equations were used. The effect of hot-phonon production on the phonon lifetime and effective energy relaxation of hot electrons was investigated as a function of lattice temperature.

(Received November 16, 2013 ; accepted September 11, 2014)

Keywords: AlInN/GaN, Hot electron, Phonon lifetime, Energy relaxation

1. Introduction

In recent decades, wide gap nitride heterostructures have been the object of intensive study. This is a consequence of the realization of the possibility of growing satisfactory samples, in turn leading to the development of high-power, high frequency and high-temperature electronics due to their larger bandgap, high breakdown field, high spontaneous and piezoelectric polarization [1-7]. These properties, together with high carrier density without doping and low sheet resistance, make the lattice matched AlInN/AlN/GaN structures ideal for the realization of a heterostructure field effect transistor [8-10]. However, from the epitaxial point of view, there exists a major difficulty in growing an AlInN based structure because the growth of AlN and InN requires different growth temperatures. Therefore, the formation of AlInN with the variance of composition in a controlled way is not straightforward. However, reports on AlInN and AlInN/GaN heterostructures in literature are rapidly increasing [11-13]. In order to analyze and improve the design of functional devices and further predict the novel devices based on these materials, understanding hot electron transport is necessary. The operation of these heterostructure devices depends on the hot-electron transport and the power dissipation controlled by hot-electron temperature.

Electron–longitudinal optical (LO) phonon interaction is among the main scattering mechanisms responsible for hot electron effects and can provide valuable information about the nature of transport properties of the electronic systems of modern semiconductors [14]. Due to electron–LO-phonon interaction in nitrides, a large part of the supplied power is transferred to the LO phonon system [15]. Hot phonon lifetime is introduced; it depends on ambient temperature [16] and carrier density [17]. The hot phonon lifetime has been measured using different techniques [18]. For the AlInN/AlN/GaN, the phonon lifetime decreases from 0.8 ps to 0.15 ps depending on the hot phonon temperature at an electron density of $1.2x10^{13}$ cm^{-3} using the microwave noise technique at 291 K [11]. The hot-electron energy relaxation times for the AlInN/AlN/GaN two dimensional electron gas (2DEG) channel were found ~ 6 ps and 75 ± 20 fs for the supplied power of P < 2 nW/electron and P ≈ 200 nW/electron, respectively [11]. Hot phonon lifetime is found to be approx. 0.65 ps at 293K for the lattice-matched InAlN/AlN/GaN structure using the same technique [19]. In other work of the same group, the hot phonon lifetime is found to be 0.27 ps for lower supplied power and decrease to 30±15 fs for the supplied power between 10 and 100 nW/electron with a sheet density of $8x10^{12}$ cm^{-2} at room temperature in InAlN/AlN/GaN heterostructures [20]. For a sheet density of $1.2x10^{13}$ cm^{-2}, the phonon lifetime is

found to be ~ 600 fs and ~ 80 fs for P~10 nW/electron and P~100 nW/electron, respectively, at room temperature in InAlN/AlN/GaN [21]. Phonon lifetime is 0.08 ps for 10 nW/electron, is 0.03 ps for 20 nW/electron and is 0.06 ps for 50 nW/electron with a sheet density of 0.8 x10^{13} cm^{-2} in InAlN/AlN/GaN [22]. One can conclude that the energy relaxation time and phonon lifetime strongly depend on the supplied power and sheet carrier density.

In spite of experimental and theoretical advancements, there are only a limited number of hot electron studies in AlInN/GaN HEMT structures. The dependence of hot electron transport on lattice temperature has not been studied. In the present work, a relatively simple method, the so-called mobility comparison technique, together with the power balance conditions as described by N.Balkan et al. [23], is used to obtain the electron temperatures as a function of an applied electric field and the electron energy loss rate as a function of the electron temperature.

2. Experimental details and results

2.1 Hall measurements

The AlInN/AlN/GaN samples were grown on *c*-plane (0001) sapphire (Al_2O_3) substrates in a low-pressure MOCVD [24]. Trimethylgallium (TMGa), trimethylaluminum (TMAl), trimethylindium (TMIn), and ammonia (NH_3) were used as Ga, Al, In, and N precursors, respectively. The growth of HEMT structures was initiated with a 15-nm-thick low temperature AlN nucleation layer at a temperature of 650°C. Then, a 0.5 µm thick high temperature (HT) AlN buffer layer was grown at 1150°C. A 2 µm thick nominally undoped GaN layer was then grown at 1050°C. In order to reduce alloy disorder scattering, a 1.2–1.3 nm thick HT AlN spacer layer was grown at a temperature of 1150°C. AlInN barrier layers were deposited on an AlN spacer layer at growth temperatures of 800°C. The growth was finished by growing a 3 nm thick GaN cap layer at a temperature of 1050°C.

Hall measurements were carried out using Van der Pauw geometry. Indium was annealed onto the sample to provide ohmic contacts. During the Hall measurements, the current supply through the sample was deliberately kept low to ensure ohmic condition; hence, the 2DEG was in thermal equilibrium with the lattice. The Hall measurements were performed at temperatures between 30K and 300K using a variable temperature cryostat and electromagnet assembly.

Fig. 1 shows the temperature dependent Hall mobilities and electron density of the AlInN/AlN/GaN heterostructures grown on sapphire. Since the Hall data could not be produced above 300 K due to the limitation of the experimental setup, possible mobility values were deduced by applying a theoretical fit that includes main scattering processes, such as acoustic and optical phonon scattering, interface roughness, background impurity scatterings. These data were used to extract the electron temperature in the mobility comparison method. The excellent agreement of the theoretical and experimental mobility data below room temperature encourages us to use the expected mobility values at temperatures above 300 K. The sample designed with an $Al_{0.88}In_{0.12}N$ barrier exhibited a very high sheet electron density of 4.84×10^{13} cm^{-2} with a corresponding electron mobility of 724 cm^2 / V.s at room temperature. The observed high 2DEG density was attributed to the larger polarization fields [25]. A record two-dimensional sheet resistance of 182 Ω/sq was obtained in the sample. This achievement was due to the improvement in the quality of the epilayers and the high sheet carrier density at the heterointerface.

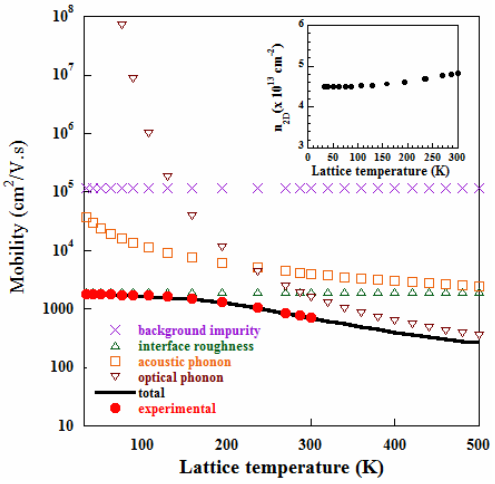

Fig. 1. The lattice temperature evolution of the measured Hall mobility and theoretical mobility including interface roughness scattering, background impurity scattering, acoustic and optical phonon scatterings. The inset in the graphic shows the variation of the 2DEG density with lattice temperatures.

2.2 I-V measurements

For pulsed I-V measurements, a simple bar geometry with length L = 48 µm and width w = 5 µm was used. Short bias pulses were applied to minimize Joule heating. In these measurements, voltage pulses of 400 ns duration were applied along the length of the sample up to a maximum electric field of E=23 kV/cm. Both the applied voltage and current through the sample were measured using a 500 MHz oscilloscope.

Fig. 2 shows the pulsed I–V plot measured at lattice temperatures range from 10 K to 300 K. The resistance is ohmic at applied voltages V < 10 V. At higher voltages, the I–V characteristic become non-linear, as would be expected from the increased interaction of hot electrons with LO phonons. Towards high voltages (V > 100 V) the current reaches I ≈ 24 mA and 22.5 mA at lattice temperatures T_L = 10 K and 300 K, respectively.

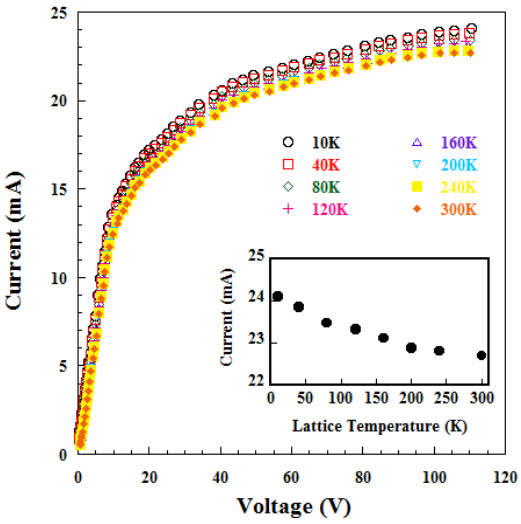

Fig. 2. Pulsed current–voltage measurements at different lattice temperatures for the AlInN/AlN/GaN HEMT structure grown on sapphire substrate. The inset in the graphic shows the variation of the current with lattice temperatures at an electric field of 23 kV/cm.

Fig. 3 shows the dependence of electron drift velocity on electric field for AlInN/AlN/GaN heterostructure at different temperatures. Electric field and drift velocity are calculated from the current–voltage characteristics. At low fields, the drift velocity exhibits linear behavior, but at higher fields (> 4 kV) it deviates linearity. When the effect of Joule heating is minimized through the application of nanosecond pulses of voltage, no velocity saturation is reached at fields up to 23 kV/cm. At electric field of 23 kV/cm the estimated drift velocity is approx. 6.69×10^6 cm/s and 6.06×10^6 cm/s at T_L = 10K and 300K, respectively.

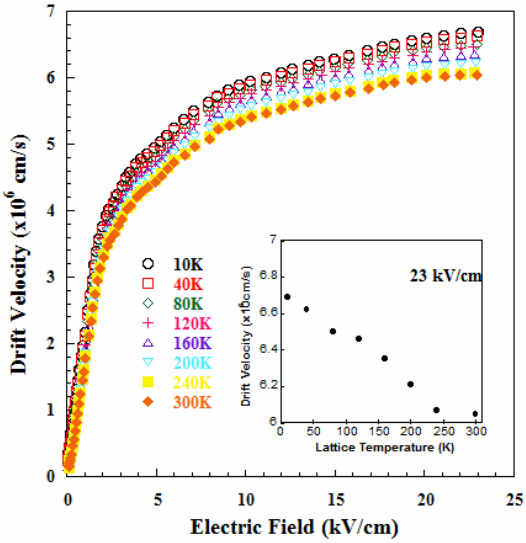

Fig. 3. Dependence of drift velocity on electric field for the sample at different lattice temperatures. The inset in the graphic shows the variation of the drift velocity with lattice temperatures at an electric field of 23 kV/cm.

3. Mobility comparison method

In the present work, we investigated and compared the hot electron dynamics of the AlInN/AlN/GaN HEMT structure grown by MOCVD on sapphire using the mobility comparison method with power balance equations. This method was also successfully used for GaAs [26, 27], bulk GaN [28, 29], and two dimensional AlGaN HEMT structures [23]. It involves the measurement of both the electric field dependence of the mobility (μ_E) at a fixed lattice temperature, and the lattice temperature dependence of the mobility at a fixed low electric field. Two sets of results are then normalized with respect to low-field mobility and low-temperature mobility, respectively. By comparing two plots, it is possible to obtain the electron temperature as a function of the electric field.

The electron temperatures obtained from the mobility comparison method for the AlInN/AlN/GaN heterostructures are shown in Fig. 4. Because of the absence of Hall data above 300 K, Hall mobility versus temperature data calculated with Matthiessen's rule was used by taking into account the dominant scattering mechanisms. As seen in the figure, the electron temperatures increase with increasing field for all lattice temperatures. As seen in the inset of Fig. 4 at the highest electric field possible the electron temperature increases monotically from 500 K to 610 K as the lattice temperature increases. The dependence of the mobility that includes active scattering mechanisms on the electron temperature is plotted in Fig. 5 at 80 K lattice temperature. This dependence of mobility is similar to the dependence of mobility on lattice temperature. Since the Hall data could not be produced above 300 K due to the limitation of the experimental setup, possible mobility values were deduced by applying a theoretical fit that includes main scattering processes, such as acoustic and optical phonon scattering, interface roughness, background impurity scatterings.

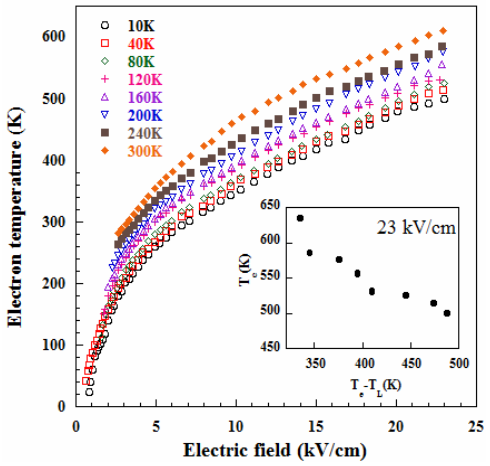

Fig. 4. Electron temperature versus the electric field at different lattice temperatures in AlInN/AlN/GaN HEMT structure. The inset in the graphic shows the variation of the electron temperature with lattice temperatures at an electric field of 23 kV/cm.

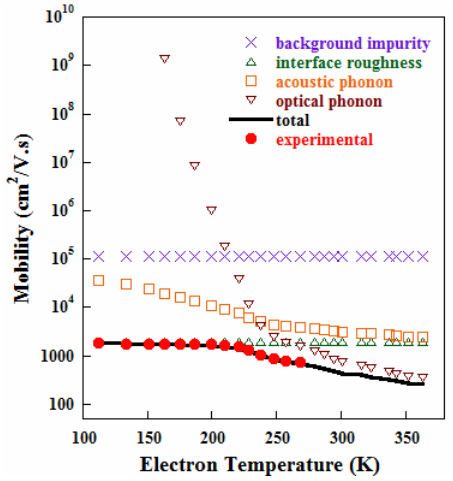

Fig. 5. The electron temperature evolution of the estimated field-dependent mobility and theoretical mobility including interface roughness scattering, background impurity scattering, acoustic and optical phonon scatterings at 80 K lattice temperature.

In the steady state, the input power is equal to the power loss to the lattice through scattering processes. Therefore, electron energy loss mechanisms and rates can be determined from the electron temperature dependence of the power loss using the power balance equations [23].

$$p = e\vartheta E \tag{1}$$

where ϑ is the electron drift velocity. At high electric fields, the electrons relax emitting LO phonons and thus reduce in energy and momentum. An expression for the power loss due to optical phonons emission and absorption can be written in the form

$$p = \frac{\hbar\omega}{\tau_0}\left[exp\left(\frac{-\hbar\omega}{k_B T_E}\right) - exp\left(\frac{-\hbar\omega}{k_B T_L}\right)\right] \tag{2}$$

where $\hbar\omega$ is the LO phonon energy, k_B is the Boltzmann constant, T_E is electron temperature, T_L is lattice temperature and τ_o is the time constant for the e-LO interaction:

$$\tau_o = \left[\frac{e^2\omega}{2\pi\hbar}\left(\frac{m^*}{2\hbar\omega}\right)^{1/2}\left(\frac{1}{\varepsilon_\infty} - \frac{1}{\varepsilon_S}\right)\right]^{-1} \tag{3}$$

where $\hbar$ is the reduced Planck constant, m^* is the effective mass of the electrons, ε_∞ and ε_s are the high frequency and static permittivities, and. Taking for GaN $m^*=0.22m_o$, $\varepsilon_\infty=5.35\varepsilon_o$, $\varepsilon_s=9.7\varepsilon_o$ and the e–LO phonon energy $\hbar\omega$ = 92 meV, we find the scattering time τ_o=8 fs. In order to take into account the hot phonon effects Eq.(2) can be modified as follows [30]:

$$p = \frac{\hbar\omega}{\tau_{eff}}\left[exp\left(\frac{-\hbar\omega}{kT_E}\right) - exp\left(\frac{-\hbar\omega}{kT_L}\right)\right] \tag{4}$$

where effective energy relaxation time τ_{eff} is the average time required by the excited electrons (hot electrons) to return to equilibrium with lattice through scattering processes. For intrasubband scattering in a deep quantum well via the interaction LO phonons in the non-degenerate case the effective energy relaxation time [23,30]

$$\tau_{eff} = \tau_{02D}(1+\gamma) \tag{5}$$

where τ_{02D} is the characteristic scattering time in the quantum well and E_L is the energy shift of the lowest subband in an infinitely deep quantum well. They can be expressed as

$$\tau_{02D} = \tau_0\left(\frac{\hbar\omega}{E_L}\right)^{1/2} \quad E_L = \frac{\hbar^2\pi^2}{2m^*L^2} \tag{6}$$

and

$$\gamma = \frac{\tau_p}{2\tau_0 q_0 L}\left(\frac{m k_B T_E}{\hbar\omega}\right)^{1/2}\frac{n}{N_c}\left[1 - exp\left(-\frac{\hbar\omega}{k_B T_E}\right)\right] \tag{7}$$

where τ_p is the phonon lifetime, $q_0 = \sqrt{(2m^*\hbar\omega)}/\hbar$ is the phase matching wave vector, L is the quantum well width, $n = n_{2D}/L$ is three dimensional electron density (n_{2D} is two dimensional density) and $N_c = m^* k_B T_E/\pi\hbar^2 L$ is the effective density of states.

Effective energy relaxation time takes into account all phonon effects for degenerate condition and can be expressed [23,31]

$$\tau_{eff} = \tau_{02D}\frac{E_F}{\hbar\omega}(1+\beta) \tag{8}$$

where $E_F = \frac{n_{2D}\hbar^2}{4\pi m^*}$ is the Fermi level and

$$\beta = \frac{\tau_p}{2\tau_0}\frac{1}{q_0 L}\frac{1}{\left(\frac{E_F}{\hbar\omega} - \frac{1}{2}\right)^{1/2}} \tag{9}$$

In the high-temperature regime, an expression for the power loss due to acoustic phonons emission can be expressed [32]

$$p = (C_{np} + C_p)(k_B T_E - k_B T_L) \tag{10}$$

where

$$C_{np} = \frac{3\Xi^2 m^{*2}}{2\rho\hbar^3 L} \tag{11}$$

and

$$C_p = \frac{3e^2 K_{av}^2 m^{*2} V_s^2}{4\pi\varepsilon\hbar^3 L n_{2D}} \tag{12}$$

are the magnitudes of the deformation-potential and piezoelectric interactions, respectively. Here, Ξ is the acoustic deformation potential, ρ is the material density, V_s is the speed of sound in the material, and K_{av} is the average electromechanical coupling constant. In the

calculations of power loss due to acoustic phonons emission we used Ξ=8.3 eV, ρ=6.15x10^3 kg/m^3, L = 65 Å, V_s = 2.16x10^3 m/s, K_{av}^2= 0.039 for GaN.

The experimentally obtained power loss per electron versus the electron temperature of the AlInN/AlN/GaN heterostructure at 80 K lattice temperature is plotted in Fig. 6. Theoretical power loss rates that do not include the hot-phonon effects are also shown in the figure. Since a large extent of disagreement with our experimental results is observed, the non-drifting hot-phonon effects were also taken into account for non-degenerate and degenerate case. The solid line represents theoretical power loss per electron via acoustic phonons and optical phonons in degenerate case including hot phonon effects**.** The reason for the observed disagreement between the experimental and theoretical loss rates at low electron temperatures might be due to the ineffectiveness of the hot phonon effect. On the other hand, excellent agreement was realized between the experimental and theoretical power loss rates at higher electron temperature regimes where the optical phonon scattering is expected to be more effective in the energy relaxation mechanism for all lattice temperatures.

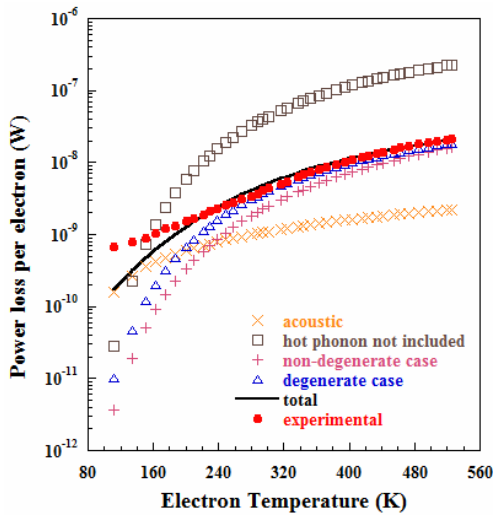

Fig. 6. Power loss per electron versus an electron temperature at 80 K lattice temperature for non-degenerate and degenerate cases. Cross: Theoretical power loss via acoustic phonon emission. Square: Hot phonon not included theoretical power loss. Plus: Hot phonon included theoretical power loss for non-degenerate condition. Triangle: Hot phonon included theoretical power loss for degenerate condition. Line: Theoretical power loss per electron via acoustic phonons and optical phonons. Circles: Experimental power loss per electron.

The dependence of the hot-electron energy relaxation time and hot phonon lifetime on the lattice temperature for the first time has been extracted for the highest field achieved during the measurements. The variation of the effective energy relaxation time with lattice temperature calculated using equation (5) is plotted in Fig. 7 for non-degenerate condition. As a result of the high effective density of states the non-degenerate condition is expected to be reached at very high electron temperatures where the effective energy relaxation time depends on the electron temperature. We have also calculated the effective energy relaxation time using equation (5) for the degenerate case as shown in Fig. 7. Supposing that we ignore the subband structure of the quantum well channel, the experimental results yield the values for the hot-electron energy relaxation time in the range 150–200 fs for non-degenerate and 90-105 fs for degenerate cases, respectively**.**

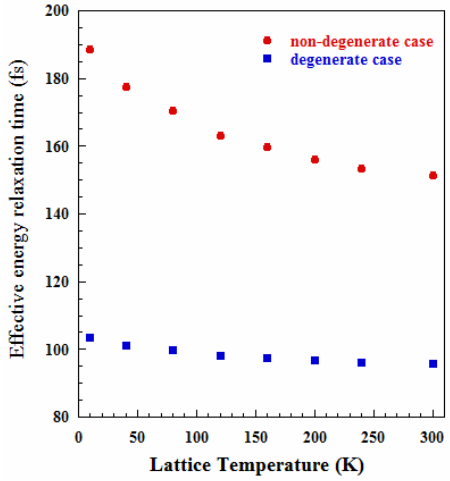

Fig. 7. Dependence of the hot-electron energy relaxation time on the lattice temperature for the AlInN/AlN/GaN 2DEG channel for non-degenerate and degenerate conditions.

Fig. 8 shows theoretical and experimental LO-phonon lifetimes as a function of lattice temperature. From theoretical view point, the lifetime of phonons generated during carrier relaxation in AlInN/AlN/GaN heterostructure can be controlled by decay of the optical phonon modes at low and high temperatures.

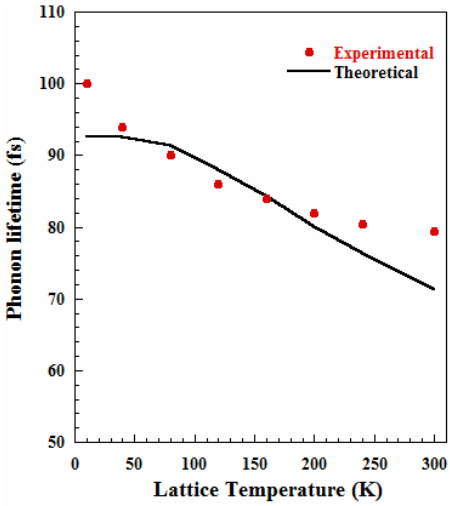

Fig. 8. Dependence of the experimental and theoretical hot phonon lifetime on the lattice temperature for the AlInN/AlN/GaN 2DEG channel at an electric field of 23 kV/cm.

The experimental hot-phonon lifetime is found to be in the range of 80-100 fs. A long wavelength optical phonon mode can decay into lower energy optical and/or acoustic modes dictated by energy and momentum conservation conditions in wurtzite GaN [33]. The decay of the optical phonon mode into a lower-branch optical mode (TO) and an acoustic mode (LA or TA) is known as the Ridley channel [34] and it can be expressed as

$$\tau^{-1}[SO \rightarrow S'O + S''A] = \frac{A\hbar\gamma^2}{4\pi\rho c'^2 c^3_{S''A}} \omega^3_{S''A} \omega_{SO} \omega_{S'O} \frac{n'(\omega_{S'O}) n'(\omega_{S''A})}{n'(\omega_{SO})} \quad (13)$$

where S, S', S''=L or T and $\omega_{S''A} = \omega_{SO} - \omega_{S'O}$. For Ridley channel: LO→TO+LA or LO→TO+TA. Our sample has very high sheet electron density of 4.84×10^{13} cm^{-2} compared to literature. Thus we considered A=0.45 as an adjustable parameter in this study. c' is the average acoustic phonon speed, γ is the mode-average Grüneisen's constant. $c_{S''A}$ is LA or TA phonon speed, $\omega_{S''A}, \omega_{SO}, \omega_{S'O}$ are characteristic phonon frequencies. $n'(\omega_{SO})$ etc. represent the Bose-Einstein distribution function for the phonon modes SO, etc. In addition to phonon decay process, the scattering rate of a phonon of frequency ω from impurities, defects, roughness can be calculated by using the Rayleigh Formula $\tau^{-1} = B\omega^4 = 0.0147\text{x}10^{12}\ s^{-1}$ [33]. Nature of impurities, defects, roughness of the samples studied here is not fully established. Thus we used B= $4\text{x}10^{-47}$. Because the mobility comparison is an indirect method the agreement between experimental and theoretical lifetimes [34] could not be realized as shown in Fig. 8. As stated in literature, from theoretical point of view, the lifetime of the phonons generated during carrier relaxation in semiconductors can be controlled by various sources such as impurity scattering, carrier scattering and anharmonic scattering from other phonons. For high quality single crystals phonon-impurity scattering can be neglected. Also, observed phonon lifetimes (in the ps range) are usually much larger than that predicted from carrier phonon interaction (in the fs range) [35]. Thus it is assumed that lifetime of such phonons is almost exclusively contributed by anharmonic interactions in the form of decay into phonons of lower energies. For grown samples, however, the low temperature phonon lifetimes may also be influenced by roughness scattering [33].

4. Conclusions

We studied the hot electron transport of AlInN/AlN/GaN HEMT structures with a high sheet electron density of 4.84×10^{13} cm^{-2} grown by MOCVD on sapphire substrates over the temperature range 10 K–300 K using the mobility comparison method with power balance equations. Current-voltage characteristics show that current and drift velocity increase linearly but deviate from the linearity towards high voltages, as would be expected from the increased scattering of hot electrons with LO phonons. However, no saturation of the current and drift velocity are observed at high voltages. Drift velocities are deduced as approximately 6.69×10^6 and 6.06×10^6 cm/s at an electric field of around E ~ 23 kV/cm at lattice temperatures T_L = 10K and 300 K. To obtain the electron temperature as a function of the applied electric field and power loss as a function of the electron temperature, we used the so-called mobility comparison method with power balance equations. The electron temperatures obtained for a 300K lattice temperature are higher than for 10 K at the same electric field. The effective energy relaxation times and phonon lifetimes are investigated as a function of lattice temperature. Supposing that we ignore the subband structure of the quantum well channel, the hot-electron energy relaxation time is found in the range 150–200 fs for non-degenerate and 90-105 fs for degenerate cases at the studied lattice temperature range. The hot-phonon lifetime is obtained in the range of 80-100 fs.

References

[1] H. Morkoc, Handbook of Nitride Semiconductors and Devices (Berlin: Springer) 2008.
[2] J. Kuzmik, IEEE Electron Device Lett., **22,** 510 (2001).
[3] O. Ambacher et al, J. Appl. Phys., **85,** 3222 (1999).
[4] S. J. Pearton, J. C. Zolper, R. J. Shul, F. Ren, J. Appl. Phys., **86,** 1 (1999).
[5] S. Nakamura, G. Fasol, The Blue Laser Diode, Springer Verlag, Berlin, 1997.
[6] S. T. Sheppard, K. Doverspike, W. L. Pribble, S. T. Allen, J. W. Palmour, L. T. Kehias, T. J. Jenkins, IEEE.Trans. Electron Devices Lett., **20,** 161 (1999).
[7] S. Strite, H. Morkoc¸ J. Vac. Sci. Technol. B **10,** 1237 (1992).
[8] J. Kuzmik, G. Pozzovivo, S. Abermann, J.F. Carlin, M. Gonshorek, E. Feltin, N. Grandjean, E. Bertagnolli, G. Strasser, D. Pogany, IEEE Trans. Electron Devices **55,** 937 (2008).
[9] A. Dadgar, M. Neuburger, F. Schulze, J. Bläsing, A. Krtschil, I. Daumiller, M. Kunze, K. M. Günther, H. Witte, A. Diez, E. Kohn, A. Krost, Phys. Status Solidi a, **202,** 832 (2005).
[10] F. Medjdoub, M. Alomari, J.-F. Carlin, M. Gonshorek, E. Feltin, M. A. Py, C. Gaquiere, N. Grandjean, E. Kohn, Electron. Lett., **44,** 696 (2008).
[11] A. Matulionis, J. Liberis, E. Šermukšnis, J. Xie, J. H. Leach, M. Wu, H. Morkoc¸ Semicond. Sci. Technol., **23,** 075048 (2008).
[12] L. Ardaravičius, M. Ramonas, J. Liberis, O. Kiprijanovič, A. Matulionis, J. Xie, M. Wu, J. H.

Leach, H. Morkoç, J. Appl. Phys., **106,** 073708 (2009).
[13] A. Teke, S. Gokden, R. Tulek, J. H. Leach, Q. Fan, J. Xie, U. Özgür, H. Morkoç, S.B. Lisesivdin, E. Özbay, New Journal of Physics, **11,** 063031 (2009).
[14] M. Ari, O.Turkoglu, Physica B, **348,** 272 (2004).
[15] A. Matulionis, J. Phys.: Condens. Matter, **21,** 174203 (2009).
[16] K. T. Tsen, D. K. Ferry, A. Botchkarev, B. Sverdlov, A. Salvador, H. Morkoç, Appl. Phys. Lett., **72,** 2132 (1998).
[17] K. T. Tsen, J. G. Kiang, D. K. Ferry, H. Morkoc, Appl. Phys. Lett., **89,** 112111 (2006).
[18] Z. Wang, K. Reimann, M. Woerner, T. Elsaesser, D. Hofstetter, J. Hwang, W. J. Schaff, L. F. Eastman, Phys. Rev. Lett., **94,** 037403 (2005).
[19] J. Liberis, I. Matulioniene, A. Matulionis, E. Šermukšnis, J. Xie, J. H. Leach, H. Morkoç, Phys. Status Solidi a, **206**(7) 1385 (2009).
[20] A. Matulionis, J. Liberis, I. Matulionienė, M. Ramonas, E. Šermukšnis, J. H. Leach, M. Wu, X. Ni, X. Li, H. Morkoç, Appl. Phys. Lett., **95,** 192102 (2009).
[21] A. Matulionis, J. Liberis, I. Matulionienė, M. Ramonas, E. Šermukšnis, Special issue on GaN and ZnO Materials and Devices of Proceedings IEEE, **98**(7), 1118 (2010).
[22] J. H. Leach, C. Y. Zhu, M. Wu, X. Ni, X. Li, J. Xie, Ü. Özgür, H. Morkoç, J. Liberis, E. Šermukšnis, A. Matulionis, T. Paskova, E. Preble, K. R. Evans, Appl. Phys. Lett. **96,** 133505 (2010).
[23] N. Balkan, M. C. Arikan, S. Gokden, V. Tilak, B. Schaff, R. J. Shealy, J. Phys.: Condens. Matter **14,** 3457 (2002).
[24] H. B. Yu, D. Çalışkan, E. Özbay, J. Appl. Phys., **100,** 033501 (2006).
[25] R. Tülek, A. Ilgaz, S. Gökden, A. Teke, M. K. Özturk, M. Kasap, S. Ozcelik, E. Arslan, E. Özbay, J. Appl. Phys. **105,** 013707 (2009).
[26] N. Balkan, R. Gupta, M. E. Daniels, B. K. Ridley, M. Emeny, Semicond. Sci. Technol. **5,** 986 (1990).
[27] R. Gupta, N. Balkan, B. K. Ridley, Semicond. Sci. Technol. **7,** 274 (1992).
[28] N. M. Stanton, A. J. Kent, A. V. Akimov, P. Hawker, T. S. Cheng, C. T. Foxon, J. Appl. Phys. **89,** 973 (2001).
[29] N. M. Stanton, A. J. Kent, A. V. Akimov, P. Hawker, T. S. Cheng, C. T. Foxon, Phys. Status Solidi a, **176,** 369 (1999).
[30] B. K. Ridley, Semicond. Sci. Technol. **4**, 1142 (1989).
[31] N. Balkan, R. Gupta, M. E. Daniels, B. K. Ridley, M. Emeny, Semicond. Sci. Technol. **5**, 986 (1990).
[32] M. Cankurtaran, H. Çelik, N. Balkan, Phys. stat. sol. (b) **229**(3), 1191 (2002).
[33] G. P. Srivastava, J. Phys.: Condens. Matter, **21,** 174205 (2009).
[34] S. Barman, G. P. Srivastava, Phys.Rev.B, **69,** 235208 (2004).
[35] J. A. Kash, J. C. Tsang, J. M. Hvam, Phys. Rev. Lett. **54,** 2151 (1985).

*Corresponding author: sozalp@balikesir.edu.tr